technical note technical note

Two-Dimensional Model of Burning for Pyrolyzable Solids

March 2013

DOT/FAA/TC-TN12/59

U.S. Department of Transportation

Federal Aviation Administration

NOTICE

Technical Report Documentation Page

1. Report No.	2. Government Accession No.	3. Recipient's Catalog No.
DOT/FAA/TC-TN12/59		

4. Title and Subtitle	5. Report Date
TWO-DIMENSIONAL MODEL OF BURNING FOR PYROLYZABLE SOLIDS	March 2013
	6. Performing Organization Code

7. Author(s)	8. Performing Organization Report No.
Stanislav I. Stoliarov*, Isaac T. Leventon*, Richard E. Lyon	

9. Performing Organization Name and Address	10. Work Unit No. (TRAIS)
*University of Maryland Department of Fire Protection Engineering 3104C J.M. Patterson Bldg. College Park, MD 20742 Federal Aviation Administration William J. Hughes Technical Center Airport and Aircraft Safety Research and Development Division Fire Safety Branch Atlantic City International Airport, NJ 08405	
	11. Contract or Grant No.

12. Sponsoring Agency Name and Address	13. Type of Report and Period Covered
U.S. Department of Transportation Federal Aviation Administration Northwest Mountain Region—Transport Airplane Directorate 1601 Lind Avenue SW Renton, WA 98057	Technical Note
	14. Sponsoring Agency Code ANM-115

15. Supplementary Notes

The Federal Aviation Administration William J. Hughes Technical Center Technical Monitor was Dr. Richard E. Lyon.

16. Abstract

A quantitative understanding of the processes that take place inside a burning material is critical for predicting the ignition and growth of fires. To improve this understanding and enable predictive modeling, a numerical pyrolysis solver called ThermaKin was developed. This solver computes the transient rate of gaseous fuel production from fundamental physical and chemical properties of constituents of a pyrolyzing solid. It was successfully applied to the combustion simulation of a broad range of materials. One limitation of ThermaKin was that it could handle only one-dimensional burning problems. As a consequence, flame spread, which is an important contributor to fire growth, could not be simulated. This technical note presents a new computational tool, ThermaKin2D, that expands the ThermaKin model to two dimensions and combines it with a flexible analytical representation of a surface flame. It is expected that this tool will enable highly accurate simulations of flame-spread dynamics. This technical note contains a description of this new computation tool, reports results of a series of verification exercises, and demonstrates some of the ThermaKin2D capabilities.

17. Key Words	18. Distribution Statement
Material flammability; Pyrolysis modeling; Burning rate; Flame spread; Fire growth; ThermaKin; ThermaKin2D	This document is available to the U.S. public through the National Technical Information Service (NTIS), Springfield, Virginia 22161. This document is also available from the Federal Aviation Administration William J. Hughes Technical Center at actlibrary.tc.faa.gov.

19. Security Classif. (of this report)	20. Security Classif. (of this page)	21. No. of Pages	22. Price
Unclassified	Unclassified	44	

TABLE OF CONTENTS

LIST OF FIGURES

LIST OF TABLES

LIST OF SYMBOLS AND ACRONYMS

1D	One-dimensional
2D	Two-dimensional
a	Parameter used to define mass flux across a boundary [m s^{-1} or kg m^{-2} s^{-1}]
A	Arrhenius pre-exponential factor [kg^{-1} m^3 s^{-1} or s^{-1}]
b	Parameter used to define mass flux across a boundary [- or J mol^{-1}]
c	Heat capacity [J kg^{-1} K^{-1}]
CI	Criterion used to define the relationship between boundary mass and heat fluxes
D	Spatial distribution used to define boundary heat flux
D_f	Spatial distribution used to define boundary heat flux related to mass fluxes
E	Arrhenius activation energy [J mol^{-1}]
h	Heat of reaction [J kg^{-1}]
hc	Convection coefficient [W m^{-2} K^{-1}]
I	Radiative heat flux [W m^{-2}]
J	Mass flux [kg m^{-2} s^{-1}]
k	Thermal conductivity [W m^{-1} K^{-1}]
mf	Mass fraction
N	Number of components
Nr	Number of reactions
P	Pressure [Pa]
q	Conductive or convective heat flux [W m^{-2}]
r	Rate of reaction [kg m^{-3} s^{-1}]
R	Molar gas constant [J mol^{-1} K^{-1}]
t	Time [s]
T	Temperature [K]
v	Fractional volume
x	Cartesian coordinate [m]
X	Object thickness [m]
y	Cartesian coordinate [m]
Y	Object length [m]
Y_f	Length scale used to define boundary heat flux related to mass fluxes [m]
α	Absorption coefficient [m^2 kg^{-1}]
β	Parameter used in the calculation of material thermal conductivity
γ	Swelling factor
ε	Emissivity
ζ	Reactant or product consumption index
θ	Stoichiometric coefficient
λ	Gas transfer coefficient [m^2 s^{-1}]
Λ	Parameter used in the definition of spatial distribution D_f
ξ	Mass-based concentration [kg m^{-3}]
ρ	Density [kg m^{-3}]
σ	Stefan-Boltzmann constant [W m^{-2} K^{-4}]
τ	Parameter used in the calculation of material swelling factor
ϕ	Volume fraction of material occupied by gases

Δx	Controlled volume (or element) thickness [m]
Δy	Controlled volume (or element) length [m]
Δt	Timestep [s]

EXECUTIVE SUMMARY

A quantitative understanding of the processes that take place inside a burning material is critical for predicting the ignition and growth of fires. To improve this understanding and enable predictive modeling, a numerical pyrolysis solver called ThermaKin was developed. This solver computes the transient rate of gaseous fuel production from fundamental physical and chemical properties of constituents of a pyrolyzing solid. It was successfully applied to the combustion simulation of a broad range of materials. One limitation of ThermaKin was that it could handle only one-dimensional burning problems. As a consequence, flame spread, which is an important contributor to fire growth, could not be simulated. This technical note presents a new computational tool, ThermaKin2D, that expands the ThermaKin model to two dimensions and combines it with a flexible analytical representation of a surface flame. It is expected that this tool will enable highly accurate simulations of flame-spread dynamics. This technical note contains a description of this new computation tool, reports results of a series of verification exercises, and demonstrates some of the ThermaKin2D capabilities.

INTRODUCTION

It has been recognized that the processes that take place in the condensed phase of a burning material play a pivotal role in the overall combustion [1]. A quantitative understanding of these processes is critical for prediction of ignition and growth of fires. During the past several years, a number of detailed numerical models that predict the rate of gaseous fuel production (or burning rate) from fundamental physical and chemical properties of constituents of a pyrolyzing solid have been developed. Examples of such models include Gpyro [2], solid phase solver within the Fire Dynamics Simulator [3]; and ThermaKin [4], which was developed by the Federal Aviation Administration. These models have similar capabilities—they solve transient conductive and radiative energy transfer coupled with decomposition chemistry. Gpyro and ThermaKin also include the transport of gaseous decomposition products inside the condensed phase and associated convective heat flow. The main distinctive feature of ThermaKin is a flexible kinetics solver that can handle chemical mechanisms consisting of up to 30 first- and second-order reactions (including those between two different reactants). Most of the newly designed flame-resistant materials are multicomponent polymeric systems with complex thermal degradation chemistry [5]. Thus, from the prospective of a fire-resistant material developer, ThermaKin represents the most suitable modeling tool.

ThermaKin has been successfully applied to the combustion simulation of noncharring [6] and charring polymers [7] in a cone calorimetry-type scenario [8]. In both cases, the model was parameterized using mg- and g-scale property measurement techniques. A simple, empirical formulation was employed to capture heat feedback from the surface flame. The burning rate and temperature histories of material samples exposed to a uniform radiant heat flux were predicted.

The cone calorimetry scenario was essentially one-dimensional, which made it a convenient simulation target. However, this scenario does not include the process of surface flame spread, which has been identified as a critical determinant of the rate of fire growth [9]. Flame-spread phenomenon was studied extensively by a large number of researchers, including de Ris [10]; Fernandez-Pello and Hirano [11]; Quintiere, et al. [12]; and Ito and Kashiwagi [13]. Nevertheless, the ability to predict this phenomenon from fundamental physical and chemical properties of a burning solid remains limited.

This technical note discusses a new computational tool, ThermaKin2D, which extends ThermaKin modeling framework to the simulation of flame spread. ThermaKin2D expands the condensed-phase pyrolysis model to two dimensions and combines it with a flexible analytical representation of a surface flame. The flame model is based on highly, spatially resolved measurements of the heat feedback from a flame spreading vertically on poly(methyl methacrylate) [13 and 14]. It is expected that coupling this flame model with a detailed pyrolysis solver will enable accurate simulations of the spread dynamics. This technical note contains a mathematic description of the new model, reports results of a series of verification exercises, and demonstrates some of the Thermakin2D model's capabilities.

MODEL DESCRIPTION

COMPONENTS AND REACTIONS.

In ThermaKin2D, the material is represented by a mixture of components. Up to 30 components can be specified in the current version of the program. Every component is characterized by density, heat capacity, thermal conductivity, gas transfer coefficient, emissivity, and absorption coefficient. The first four properties in this list are defined by a flexible function of temperature (T):

$$\text{property} = p_0 + p_1 T + p_2 T^n \tag{1}$$

where p_0, p_1, p_2, and n are user-specified parameters. Emissivity and absorption coefficient are defined by single (constant) values. All components are divided into three categories: solids, liquids, and gases. This categorization is used in the calculation of density of material as explained below.

The heat capacity or specific heat of material (c) is calculated as:

$$c = \sum_{i=1}^{N} mf_i c_i \tag{2}$$

where mf_i and c_i are mass fraction and heat capacity of the i-th component; and N is the number of components. The density of material (ρ) is defined by:

$$\rho = \frac{1}{\sum_{s=1}^{N_s} \frac{mf_s}{\rho_s} + \sum_{l=1}^{N_l} \frac{mf_l}{\rho_l} + \gamma \sum_{g=1}^{N_g} \frac{mf_g}{\rho_g}} \tag{3}$$

where ρ with a subscript designates component density. Subscripts s, l, and g are used to refer to solid, liquid, and gaseous components, respectively. Swelling factor γ, which may assume a value between 0 and 1, describes reaction of a volume of material to the presence of gases. When $\gamma = 0$, the presence of gases has no effect on volume. When $\gamma = 1$, gases contribute to the volume of material in accordance with their prescribed densities. The γ is calculated by volume-weighted averaging of the swelling factor specified for solids (γ_s) and liquids (γ_l):

$$\gamma = \frac{\gamma_s \sum_{s=1}^{N_s} \frac{mf_s}{\rho_s} + \gamma_l \sum_{l=1}^{N_l} \frac{mf_l}{\rho_l} + \tau \sum_{g=1}^{N_g} \frac{mf_g}{\rho_g}}{\sum_{s=1}^{N_s} \frac{mf_s}{\rho_s} + \sum_{l=1}^{N_l} \frac{mf_l}{\rho_l} + \tau \sum_{g=1}^{N_g} \frac{mf_g}{\rho_g}} \tag{4}$$

where τ is a parameter that is typically very small (τ <<1) and is used to ensure that, at the limit of very high gas content, the volume of material converges to that defined by gas densities.

Components may undergo reactions. Up to 30 reactions can be specified in the current version of the program. Each reaction may have one to two reactants and zero to two products:

$$\theta_1\,\mathrm{COMP1} + \theta_2\,\mathrm{COMP2} \rightarrow \theta_3\,\mathrm{COMP3} + \theta_4\,\mathrm{COMP4} + h \tag{5}$$

The θ_i are stoichiometric coefficients and h is the heat of reaction. Different reactions may involve the same components (i.e., reactions can be coupled in parallel or consecutive fashion). The rate of reaction (r) taking place in a unit volume of material is defined by:

$$r = A\exp\left(-\frac{E}{RT}\right)\xi_{\mathrm{COMP1}}\,\xi_{\mathrm{COMP2}} \tag{6}$$

where A and E are the Arrhenius pre-exponential factor and activation energy, respectively, and R is the molar gas constant. The ξ is the concentration of a given component expressed in the units of mass per unit volume ($\xi_{\mathrm{COMP1}} = mf_{\mathrm{COMP1}}\rho$). In the absence of the second reactant, ξ_{COMP2} is set to 1. The rate of consumption/formation of a reactant/product is calculated by multiplying r by the corresponding stoichiometric coefficient. The rate of production of heat is calculated by multiplying r by h (i.e., a positive h corresponds to an exothermic reaction). The h is defined by the same type of temperature dependence as that used for component properties (see equation 1).

The reaction description also includes specification of a lower- or upper-temperature limit. If temperature decreases below the lower limit or increases above the upper limit, the rate of reaction is set to 0. Application of this limit increases computational efficiency (reaction rates are evaluated only at the temperatures at which they are important) and facilitates usage of reactions for the description of phase transitions.

HEAT AND MASS TRANSFER.

The conduction of heat is described by Fourier's law:

$$q_x = -k\frac{\partial T}{\partial x} \tag{7}$$

where q_x is the heat flux in the direction of Cartesian coordinate x; and k is the thermal conductivity of material. The value of conductivity depends on relative amounts and spatial

distribution of components [15]. If components are stacked in uniform layers that are normal to the direction of heat flow, the thermal conductivity is:

$$k_n = \frac{1}{\sum_{i=1}^{N} \frac{v_i}{k_i}} \tag{8}$$

where k_i and v_i are the thermal conductivity and fractional volume of the i-th component (note that, when $\gamma = 0$, gaseous components do not contribute to the thermal conductivity). On the other hand, if the layers are parallel to the direction of heat flow, the thermal conductivity is:

$$k_p = \sum_{i=1}^{N} k_i v_i \tag{9}$$

For an arbitrary spatial distribution of components, the exact analytical expression of the thermal conductivity is not available. However, under the assumption that components do not affect thermal conductivities of each other, equations 8 and 9 provide lower and upper limits for the value of k. This means that the thermal conductivity of a multicomponent material can be represented as:

$$k = \beta k_p + (1-\beta) k_n \tag{10}$$

where β is a parameter that may assume a value between 0 and 1. In ThermaKin2D, this representation is used in conjunction with the assumption that a pyrolyzing material can be characterized by a single value of β.

Thermal radiation from an external source is absorbed inside the material according to a generalized version of the Beer-Lambert law:

$$\frac{\partial I_{ex}}{\partial x} = -I_{ex} \sum_{i=1}^{N} \alpha_i \xi_i \tag{11}$$

where I_{ex} is the flux of the radiation in x direction and α_i is the absorption coefficient of the i-th component. To comply with the second law of thermodynamics, the material is prescribed to reradiate energy to the environment according to:

$$\frac{\partial I_{rr}}{\partial x} = \frac{\sigma T^4}{I_{ex}^0} \frac{\partial I_{ex}}{\partial x} \tag{12}$$

where I_{rr} is the heat flux radiated by a material boundary; I_{ex}^0 is the external radiation incident onto that boundary; and σ is the Stefan-Boltzmann constant. In the case where no external

radiation is applied, I_{ex}^{0} value used in equation 12 is set to unity to produce meaningful calculation of radiative loss.

Equations 11 and 12 describe radiative exchange between a material object and environment. The radiative transfer inside the object is modeled using the conduction equation (equation 7) combined with the thermal conductivity expressed as the third power of temperature (using equation 1). This approach is referred to as radiative diffusion approximation; it has been shown to be accurate for an optically thick medium [16].

The transfer of mass is assumed to be driven by the gradient of volumetric fraction expressed through concentration:

$$J_g^x = -\rho_g \lambda \frac{\partial\left(\frac{\xi_g}{\rho_g}\right)}{\partial x} \tag{13}$$

Here, J_g^x is the mass flux of gas g in x direction. Only gaseous components are assumed to undergo this transfer. The λ is the gas transfer coefficient of material. It is calculated from the corresponding component coefficients using the same approach as that used for the thermal conductivity (see equations 8 to 10). Note that λ does not depend on the nature of gas that is being transferred (i.e., on volumetric basis, all gases subjected to the same volumetric fraction gradient are transferred at the same rate).

Application of Boyle's law, which states that the product of the pressure and volume of a fixed amount of gas is constant, transforms equation 13 into:

$$J_g^x = -\frac{\rho_g \lambda}{P^{def}} \frac{\partial\left(\phi P_g\right)}{\partial x} \tag{14}$$

where ϕ is the volume fraction of material occupied by gases; P_g is the partial pressure of gas g; and P^{def} is the pressure at which the gas density (ρ_g) is specified. This transformation helps clarify the transport model represented by equation 13. If the material expands proportionally to the volume of added gases (i.e., $\gamma > 0$ and pressure inside the material is constant), the flow of gas is a diffusion-like process. On the other hand, if material is rigid and does not expand with addition of gases (i.e., $\gamma = 0$ and ϕ is constant), the transport model assumes the form of Darcy's law, which is frequently used to describe the flow of fluids through a porous medium [17].

CONSERVATION EQUATIONS.

The material description requires mass and energy conservation statements. The momentum conservation is introduced implicitly within the gas flux formula (equation 13). The statements are formulated in terms of two Cartesian dimensions, x and y. The conservation of mass of component j is given by:

$$\frac{\partial \xi_j}{\partial t} = \sum_{i=1}^{Nr} (-1)^{\zeta_i^j} \theta_i^j r_i - \frac{\partial J_j^x}{\partial x} - \frac{\partial J_j^y}{\partial y} + \frac{\partial}{\partial x}\left(\xi_j \int_0^x \frac{1}{\rho} \frac{\partial \rho}{\partial t} dx \right) \tag{15}$$

where t is time and Nr is the number of reactions. The ζ_i^j is equal to 1 when j is an i-th reaction reactant and 2 when j is a product. The second and third terms on the right side account for gas transfer; they are present only if component j is a gas. The last term on the right side accounts for the mass transfer associated with contraction or expansion of a material object with respect to a stationary boundary positioned at $x = 0$. The object is assumed to be able to contract or expand only in one dimension (x).

The conservation of energy is expressed as follows:

$$\begin{aligned} \sum_{j=1}^{N} \xi_j c_j \frac{\partial T}{\partial t} = \sum_{j=1}^{Nr} h_i r_i - \frac{\partial q_x}{\partial x} - \frac{\partial q_y}{\partial y} - \frac{\partial I_{ex}}{\partial x} + \frac{\partial I_{rr}}{\partial x} - \\ - \sum_{g=1}^{N_g} c_g \left(J_g^x \frac{\partial T}{\partial x} + J_g^y \frac{\partial T}{\partial y} \right) + c\rho \frac{\partial T}{\partial x} \int_0^x \frac{1}{\rho} \frac{\partial \rho}{\partial t} dx \end{aligned} \tag{16}$$

Note that the radiative exchange between the material object and environment (described by I_{ex} and I_{rr}) is also assumed to be one dimensional (1D). Another key assumption in the energy conservation statement is that the rate of local heat transfer between gases and condensed phase components is infinite. This assumption is implemented in the sixth right-side term representing convective heat flow. An approximate finite rate correction to this assumption can be made by scaling gas heat capacities (c_g) downward from their real values. The last right-side term accounts for the heat transfer associated with contraction or expansion of the material object.

Some aspects of mass and energy conservation related to reactions are relaxed in ThermaKin2D to increase flexibility of the computational environment. In particular, a user is allowed to define any values of stoichiometric coefficients including those resulting in generation or consumption of mass in a reaction. The heat of reaction definition is also left to user discretion despite the fact that thermodynamics [18] requires that the heat is related to the heat capacities of the reactants and products:

$$h_T = h_{T_{ref}} + \int_{T_{ref}}^{T} \left(\theta_3 c_{\mathrm{COMP3}} + \theta_4 c_{\mathrm{COMP4}} - \theta_1 c_{\mathrm{COMP1}} - \theta_2 c_{\mathrm{COMP2}} \right) dT \tag{17}$$

Here the stoichiometry and heat capacity symbol subscripts are consistent with the reaction equation (equation 5). The h_T is the heat of reaction at the temperature of interest (T); and T_{ref} is a reference temperature at which the heat of reaction value ($h_{T_{ref}}$) was determined.

INITIAL AND BOUNDARY CONDITIONS.

The formulation of initial and boundary conditions in ThermaKin2D depends on whether a 1D or two-dimensional (2D) problem is being solved. In the case of a 1D problem, the initial (t = 0) material object is assumed to consist of slices of varying thickness, as shown in figure 1. Each slice may have a unique composition (defined through component mass fractions) and temperature. The number of slices is limited to 5×10^4. In the case of a 2D problem, the object consists of layers of varying length (see figure 1). Each layer is comprised of a stack of slices, in which initial composition and temperature are specified. The maximum number of layers is set at 1.5×10^3, which is also the maximum number of slices in each layer.

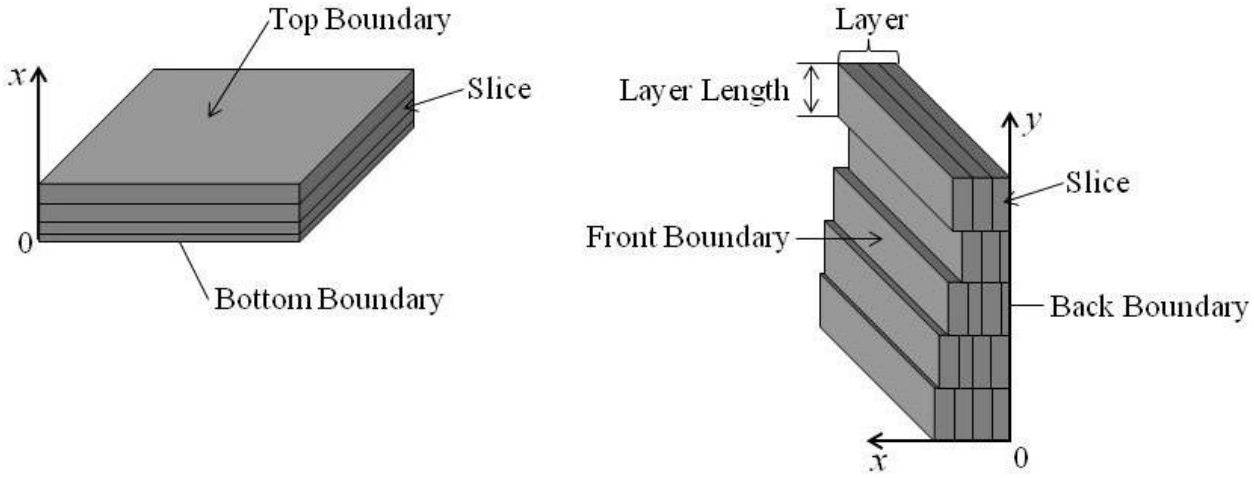

Figure 1. Structure of 1D (left) and 2D (right) Material Objects

The 1D object possesses two boundaries, top and bottom. These boundaries have unit areas and are described separately using identical mathematical frameworks. The mass flux of component i out of material object is expressed as:

$$J_i^{\mathrm{B}} = \begin{cases} a_i \rho_i^{\mathrm{B}} \left(\dfrac{\xi_i^{\mathrm{B}}}{\rho_i^{\mathrm{B}}} - b_i \right) \\ \text{or} \\ a_i \exp\left(-\dfrac{b_i}{RT^{\mathrm{B}}} \right) \end{cases} \tag{18}$$

where the B superscript indicates physical quantities at the boundary, and a_i and b_i are component-specific constants defined by a user. The primary function of the linear expression is to remove/introduce gases from/to a pyrolyzing material. The exponential expression is added to enable simulation of a surface reaction (such as oxidation) or material loss through dripping.

The convective heat flux out of a material is defined by:

$$q^{\mathrm{B}} = hc\left(T^{\mathrm{B}} - T^{\mathrm{e}}\right) \tag{19}$$

where *hc* is the convection coefficient and T^{e} is the environmental temperature, which can be specified to be a linear function of time, $T^{\mathrm{e}} = T_0^{\mathrm{e}} + T_t^{\mathrm{e}} t$. The external radiative heat flux incident onto a boundary is expressed using a piecewise-linear function of time:

$$I_{ex}^0 = \begin{cases} I_{ex}^{10} + I_{ex}^{1t} t & t \le t_1 \\ I_{ex}^{20} + I_{ex}^{2t}\left(t - t_1\right) & t_1 < t \le \left(t_1 + t_2\right) \\ I_{ex}^{20} + I_{ex}^{2t} t_2 & t > \left(t_1 + t_2\right) \end{cases} \tag{20}$$

where all *I*, t_1 and t_2 parameters on the right side are user-defined constants. Note that the superscripts do not indicate power; they are used to distinguish the parameters. This heat flux dependence can be specified to be periodic (i.e., the flux history can be repeated with a period of t_2). The external radiative heat flux through the boundary (I_{ex}^{B}) is computed by taking into account material reflectivity:

$$I_{ex}^{\mathrm{B}} = I_{ex}^0 \frac{\int_0^X \sum_{i=1}^N \varepsilon_i \nu_i I_{ex} \sum_{j=1}^N \alpha_j \xi_j dx}{\int_0^X I_{ex} \sum_{j=1}^N \alpha_j \xi_j dx} \tag{21}$$

where *X* is the object thickness and ε_i is the emissivity (or one minus reflectivity) of component *i*.

The convective and radiative heat fluxes can also be related to component mass fluxes out of material. In the case of a 1D object, these relations are based on:

$$\mathrm{CI} = \sum_{i=1}^N \frac{J_i^{\mathrm{B}}}{J_i^{\mathrm{CI}}} \tag{22}$$

where J_i^{CI} is the user-specified critical (or ignition) mass flux of component *i*. Note that only positive J_i^{B} are counted (i.e., component flows into material do not contribute to the criterion value). When CI reaches 1, a constant user-defined value is added to I_{ex}^0 and new constant values are assigned to *hc* and T^{e}. These relations are used to simulate the appearance of a flame on the material surface.

According to figure 1, a 2D object has four sides. Two of these sides are parts of the planes defined by $y = 0$ and $y = Y$, where Y is the length of the object. These planes are assumed to be impenetrable to mass and energy flow. The other two sides are referred to as front and back boundaries. The back boundary has surface area Y and is a part of the $x = 0$ plane. This boundary serves as a reference point for expansion or contraction of a 2D object. The front boundary may have a nonuniform profile due to differences in the object thickness (X of a 2D object is a function of y). In the mass and energy flow calculations, this nonuniformity is ignored; it is assumed that the boundary surface area is defined by its projection onto the $x = 0$ plane.

The front and back boundaries are described separately using identical mathematical frameworks. The mass fluxes of components out of the boundaries are defined using equation 18 (note that in the case of a 2D object, J_i^{B} is a function of y). The external heat flux is specified using a piecewise-linear-spatial distribution function:

$$D = \begin{cases} D_0^1 + D_y^1 y & y < y_1 \\ D_0^2 + D_y^2 y & y_1 \le y < y_2 \\ D_0^3 + D_y^3 y & y_2 \le y < y_3 \\ 0 & y \ge y_3 \end{cases} \tag{23}$$

where all D, y_1, y_2, and y_3 parameters on the right side are user-defined constants. Note that the numerical superscripts do not indicate power; they are used to distinguish the parameters. D can be specified to represent radiative heat flux incident onto a boundary (I_{ex}^0) or environmental temperature (T^{e}), which defines convective heat flux out of the object (in accordance with equation 19). The latter specification requires that a constant convection coefficient (hc) also be provided. Two modules for the external heat flux specification are available in ThermaKin2D. Each of these modules contains its own set of the heat flux constants and includes a definition of the start and end of exposure times.

An additional external heat flow can be specified to be related to component mass fluxes. The functional shape of this relationship is based on the measurements of energy feedback from small (2- to 20-cm-tall) flames spreading on a solid surface [13 and 14]. The spatial distribution for the heat flow is defined in terms of its own length scale:

$$Y_f = Y_f^0 + Y_f^{\mathrm{CI}} \left(\int_0^Y \mathrm{CI} dy \right)^{Y_f^{\mathrm{PW}}} \tag{24}$$

where all Y_f on the right side are user-specified constants and CI is defined by equation 22. The spatial distribution is given by:

$$D_f = \begin{cases} D_f^1 \exp\left(-D_f^3 \left(y - y_f\right)^2\right) & y < y_f \\ D_f^1 & y_f \le y < (y_f + y_f^s) \text{ and } y < (y_f + Y_f) \\ D_f^2 & (y_f + y_f^s) \le y < (y_f + Y_f) \\ D_f^1 \left(\dfrac{y - y_f}{Y_f}\right)^{-\Lambda} & y \ge (y_f + Y_f) \text{ and } y_f^s > Y_f \\ D_f^2 \left(\dfrac{y - y_f}{Y_f}\right)^{-\Lambda} & y \ge (y_f + Y_f) \text{ and } y_f^s \le Y_f \end{cases} \tag{25}$$

Here all D and y_f^s parameters on the right side are user-specified constants. Note that D superscripts do not indicate power; they are used to distinguish the parameters. The y_f designates the lowest (closest to y = 0) point on the object surface where $\mathrm{CI} \ge 1$. If no such point exists, D_f = 0. The exponent Λ is related to component mass fluxes through:

$$\Lambda = \Lambda_0 + \Lambda_{\mathrm{CI}} \exp\left(-\Lambda_{\mathrm{ex}} \int_0^Y \mathrm{CI} dy\right) \tag{26}$$

where all Λ on the right side are user-specified constants. As in the case of mass-flux-independent external heat fluxes, D_f can be specified to represent incident-radiative heat flux or environmental temperature (which defines convection). The latter specification requires that the corresponding convection coefficient is also defined. The radiative or convective heat flux specified using D_f is added to the radiative and connective heat fluxes defined through equation 23.

The last parameter describing heat flow through a 2D object boundary is a background temperature; T_b. T_b is a used-specified constant that is added to all values of environmental temperature (T^e). This temperature also defines additional radiative heat flux equal to σT_b^4 incident onto the object surface. T_b represents the equilibrium temperature of a 2D object in the absence of external heating or flame.

SOLUTION METHODOLOGY.

To solve the conservation equations described above, a material object is divided into rectangular volumes of identical dimensions. For a 1D object, the volumes (or elements) are characterized by thickness Δx. The maximum number of elements is limited to 5×10^4. For a 2D object, the elements are characterized by thickness Δx and length Δy. The Δx and Δy represent discretization in the x- and y-coordinate direction, respectively (see figure 1). The object may

contain up to 1.5×10^3 elements stacked in the *x*- and *y*-directions. Thus, the total number of elements used to describe a 2D object is limited to 2.25×10^6.

Each element is also characterized by masses of components and temperature. In the numerical formulation, these parameters represent primary object descriptors. Changes in these descriptors with time are computed using a small timestep Δt. For *x*-dimension (of 1D or 2D objects), the time integration is based on the Crank-Nicolson scheme [19]. A detailed description of this integration procedure can be found in reference 4. For the *y*-dimension, a simple explicit integration is used. The *x*-dimension of a 2D object is expected to be associated with higher temperature and concentration gradients; therefore, a more stable semi-implicit integration technique is applied to this coordinate. The *x* is also the dimension of radiative heat transfer and object deformation (see equations 16 and 15, respectively).

It should be noted that, as a result of object deformation, Δx of individual elements changes with time. These changes, accumulated over time, may have substantial negative effects on the accuracy of the solution procedure. To minimize these effects, element thicknesses are adjusted after every timestep. If an element is larger than a preset value of Δx, it is split in two. If it is smaller, a fraction of the following element is added to bring it to the preset thickness. The temperature and composition of the mixed element are recalculated to ensure the conservation of energy and species.

To simplify the solution, the radiation-related terms (terms 4 and 5 on the right side of equation 16) are incorporated into the energy conservation using either the maximum- or random-absorption algorithm. In the case of the maximum-absorption algorithm, the element that, according to equation 11, absorbs most of the external radiation is assumed to absorb all of it (corrected for reflection). In the case of the random-absorption algorithm, a Monte Carlo approach is used to distribute the radiative energy. The absorbing element is selected at random using the distribution of energy obtained from the solution of equation 11 as a probability density guiding this selection. In both cases, the element selection is performed at every timestep. Reradiation of energy to the environment is computed using temperature and emissivity of the same element that is selected to absorb (and reflect) external radiation.

ThermaKin2D is implemented using ANSI/ISO C++ and its standard library. A single instance of the program is designed to run on a single processor (or core) and may require up to several gigabytes of random-access memory (the memory requirement depends on the number of components and number of elements in the object). A brief description of the program input and output is given in the following section.

INPUT AND OUTPUT.

When the ThermaKin2D program starts, it asks for three file names. The information on components and reactions is read from the components file. The information on the initial state of a material object, boundary conditions, and integration parameters is read from the conditions file. The last name is a new file from which the calculation results are output. Both input and output files have a simple text format. The input is case sensitive. The current version of ThermaKin2D does not have any parameter-checking algorithms. It is the responsibility of the

user to make sure that (within the range of conditions encountered in a given simulation) the parameters are meaningful. The representative components and conditions files used below are examples of those employed in the burning rate simulations described in the Model Verification section.

The specification of components in ThermaKin2D (whether for 1D or 2D objects) is performed identically as in previous versions of ThermaKin. This file begins with the component's name (single word, no spaces), followed by its state (S for solid, L for liquid, or G for gas) and properties.

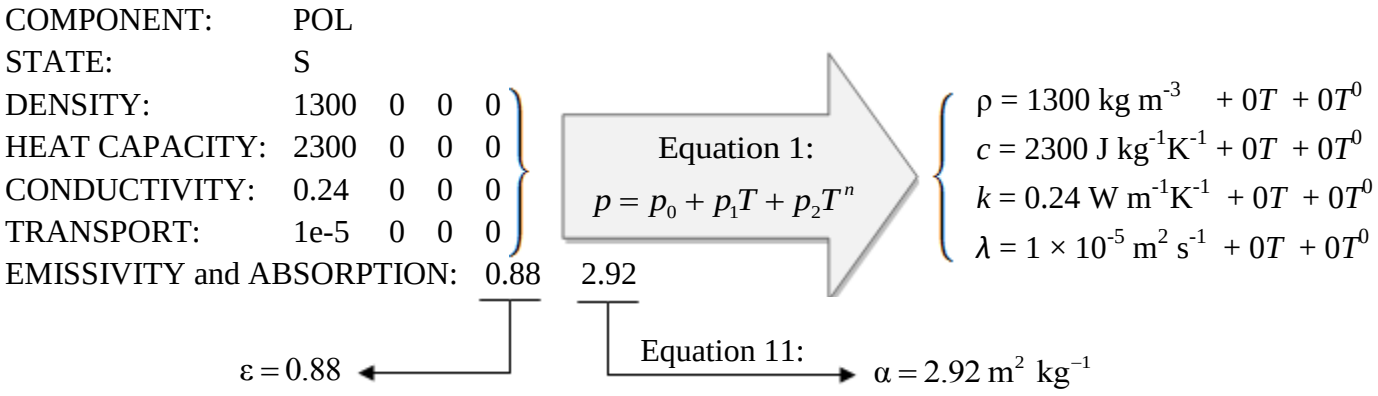

Density, heat capacity, thermal conductivity, and gas transfer coefficient (TRANSPORT) are defined by specifying parameters of equation 1 in the following order: p_0, p_1, p_2, and n. Emissivity and absorption coefficient are defined by single values. The current version of ThermaKin allows up to 30 components. Their specifications should be separated by at least one space.

Chemical reactions are defined as follows:

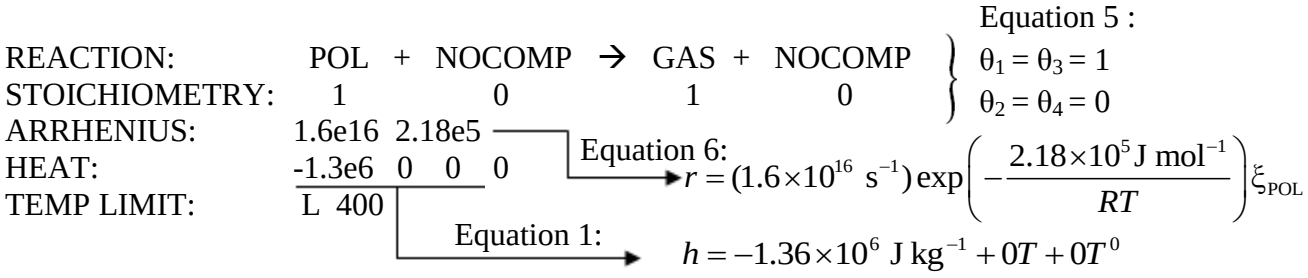

If the program encounters a component that is not specified (NOCOMP), it omits this component from the reaction definition. Stoichiometric coefficients θ (see equation 5) are specified in the same order as the corresponding component names in the reaction equation. The stoichiometry is followed by the Arrhenius parameters A and E (see equation 6). The heat of reaction (HEAT) is defined by parameters of equation 1 (p_0, p_1, p_2, and n). The last parameter in the reaction description is the upper- (U) or lower- (L) temperature limit (the limit above or below which the rate of reaction is set to 0). The current version of ThermaKin2D allows up to 30 reactions. Their specifications should be separated by at least one space.

The components file may also contain a description of physical interactions between components.

MIXTURES
S SWELLING: 0 $\longrightarrow$ $\gamma_s = 0$
L SWELLING: 0 $\longrightarrow$ $\gamma_l = 0$
G SWELLING LIMIT: 1e-30 $\longrightarrow$ $\tau = 1 \times 10^{-30}$
PARALL CONDUCTIVITY: 0.5 $\longrightarrow$ $\beta = 0.5$
PARALL TRANSPORT: 0.5 $\longrightarrow$ $\beta_\lambda = 0.5$

This description includes the values of γ_s (S SWELLING), γ_l (L SWELLING), and τ (G SWELLING LIMIT) parameters, which are used in the calculation of a material's swelling factor (see equation 4). The last two parameters in the description define the weight of parallel averaging (parameter β) in the calculations of the thermal conductivity (equation 10) and gas transfer coefficient of material.

The conditions file begins with a definition of model dimensionality followed by a specification of the initial state of the object and boundary conditions. This file is used to define either a 1D or 2D object as indicated by the file's first line, OBJECT TYPE. The conditions file for 1D objects begins with a specification of the OBJECT TYPE as 1D, followed by a definition of object structure and initial state, as shown in figure 2.

OBJECT TYPE: 1D

OBJECT STRUCTURE

THICKNESS: 0.005
TEMPERATURE: 300
MASS FRACTIONS:
POL 1

THICKNESS: 0.00025
TEMPERATURE: 300
MASS FRACTIONS:
INS 1

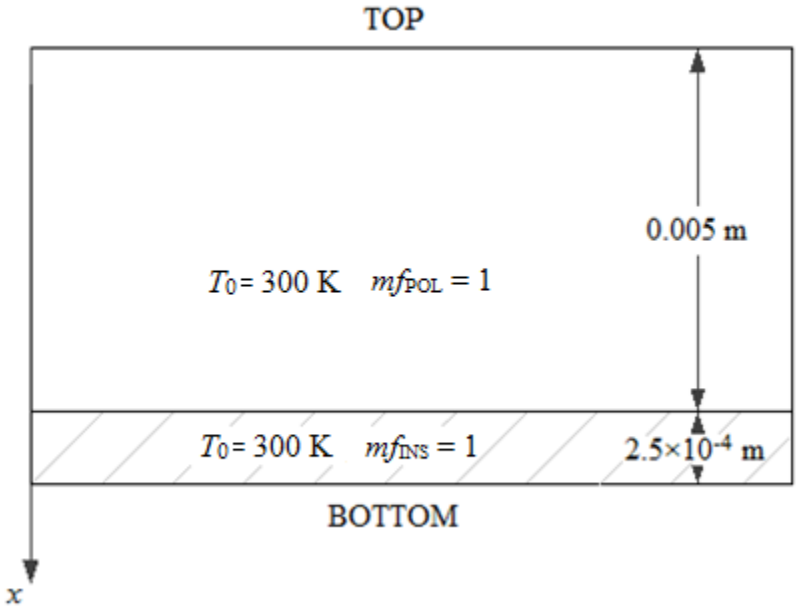

Figure 2. The 1D Object Defined by Example Conditions File

A 1D object is assumed to consist of layers. Each layer is characterized by thickness, temperature, and mass fractions of components. After the object structure, boundary conditions are defined:

OBJECT BOUNDARIES

TOP BOUNDARY
MASS TRANSPORT: YES
GAS LIN 0.05 0 → Equation 18: $J^{B}_{GAS} = 0.05\ \mathrm{m\ s^{-1}} \bullet \rho^{B}_{GAS}\left(\frac{\xi^{B}_{GAS}}{\rho^{B}_{GAS}} - 0\right)$

OUTSIDE TEMP TIME PROG: 300 0
CONVECTION COEFF: 0
} → Equation 19: $q^{B} = 0\ \mathrm{W\,m^{-1}K^{-1}}(T^{B} - 300\ \mathrm{K})$

EXTERNAL RADIATION: YES
TIME PROG1: 5e4 0 1e5
TIME PROG2: 0 0 0
REPEAT: NO
ABSORPTION MODE: RAND

Equation 20:
$I^{10}_{ex} = 5\times10^{4}\ \mathrm{W\,m^{-2}}$
$I^{1t}_{ex} = 0\ \mathrm{W\,m^{-2}\,s^{-1}} \quad t_1 = 1\times10^{5}\ \mathrm{s}$
$I^{20}_{ex} = I^{2t}_{ex} = t_2 = 0$

FLAME: NO
IGNITION MASS FLUXES:
GAS 3e-3 → $J^{CI}_{GAS} = 3\times10^{-3}\ \mathrm{kg\,m^{-2}\,s^{-1}}$
OUTSIDE TEMP: 300
CONVECTION COEFF: 0
RADIATION: 1.5e4

BOTTOM BOUNDARY

MASS TRANSPORT: NO

OUTSIDE TEMP TIME PROG: 300 0
CONVECTION COEFF: 0

EXTERNAL RADIATION: NO

FLAME: NO

The definition of the top boundary, which corresponds to the layer of material specified first in the object structure, is followed by that of the bottom boundary. These definitions have identical format. Component mass flows (MASS TRANSPORT) are defined by listing the name of component, type of expression (LIN for linear or EXP for exponential), and values of parameters *a* and *b* used in the expression (see equation 18). When exponential form of the mass flow expression is used, *b* has the units of J mol^{-1}. Turning off mass flow (MASS TRANSPORT: NO) at both boundaries also turns off mass transfer inside the object.

The convective heat flow across a boundary is defined by specifying outside temperature, T^e, and convection coefficient *hc* (see equation 19). The outside temperature is expressed as a linear function of time (OUTSIDE TEMP TIME PROG). This function is defined by the initial temperature value followed by the rate at which this temperature changes. The flux of external radiation I_{ex}^0 (see equation 20) is defined by sequence 2 linear time dependencies (TIME PROG1 and TIME PROG2). Each of these dependencies is defined by the initial flux value, the rate of change of the flux, and the length of time during which the dependence is followed. If the sequence is specified to repeat itself (REPEAT: YES), the program will do it for as long as the simulation is run. The last parameter in the external radiation specification (ABSORPTION MODE) is used to select between the maximum (MAX) and random (RAND) radiation absorption algorithms. When the external radiation is turned off (EXTERNAL RADIATION: NO), the maximum radiation-absorption algorithm is used by default.

The last set of entries defining a boundary (beginning with FLAME keyword) describes surface ignition. First, critical (IGNITION) mass fluxes J_i^{CI} (see equation 22) are listed next to the corresponding component names. Those components that are not listed are assumed to have infinite J_i^{CI}. Next, convective heat transfer parameters T^e and *hc* describing the flaming conditions are specified (T^e in this case is a constant). The last parameter (RADIATION) is the radiative heat flux from the flame. This flux is added to the external heat flux I_{ex}^0, when the flame is on.

The top and bottom boundaries are mathematically identical in all aspects, except one. When element sizes are adjusted (using an algorithm described in the Solution Methodology section), the adjustment procedure always starts from the bottom boundary element and proceeds to the top. To minimize object structure distortions caused by this procedure, the object side experiencing the most significant shrinkage or expansion should be bound by the top boundary. The conditions file is completed by specifying integration and output parameters.

INTEGRATION PARAMETERS

ELEMENT SIZE: 5e-5 $\longrightarrow$ $\Delta x = 5\times10^{-5}\,\mathrm{m}$
TIME STEP: 0.01 $\longrightarrow$ $\Delta t = 0.01\,\mathrm{s}$
DURATION: 500

OUTPUT FREQUENCY:
ELEMENTS: 10
TIME STEPS: 100

Element size, timestep, and the length (DURATION) of simulation are followed by output frequencies. In the example shown above, information on the state of the object will be output every 100 timesteps. The output will include specification of location, temperature, and composition of every tenth element of the object.

2D model objects are defined similarly as above with the following changes to the formatting of the conditions file. Objects are created from bottom (y = 0) up, by first defining a layer of set

dimension LAYER LENGTH (in the *y*-direction) and then, from front to back in the *x*-direction, defining slices of dimension THICKNESS with initial temperature and mass fractions of components defined in the components file. Additional layers can then be defined in the same order, thus allowing the user to vary object structure, initial composition, and temperature along *x*- and *y*-coordinates. The example file used below is representative of the conditions file used in upward flame-spread simulations described in the Model Verification section.

OBJECT TYPE: 2D

OBJECT STRUCTURE

FROM BOTTOM:

LAYER LENGTH: 0.15

FROM FRONT:

THICKNESS: 0.005
TEMPERATURE: 300
MASS FRACTIONS:
POL 1

THICKNESS: 0.00025
TEMPERATURE: 300
MASS FRACTIONS:
INS 1

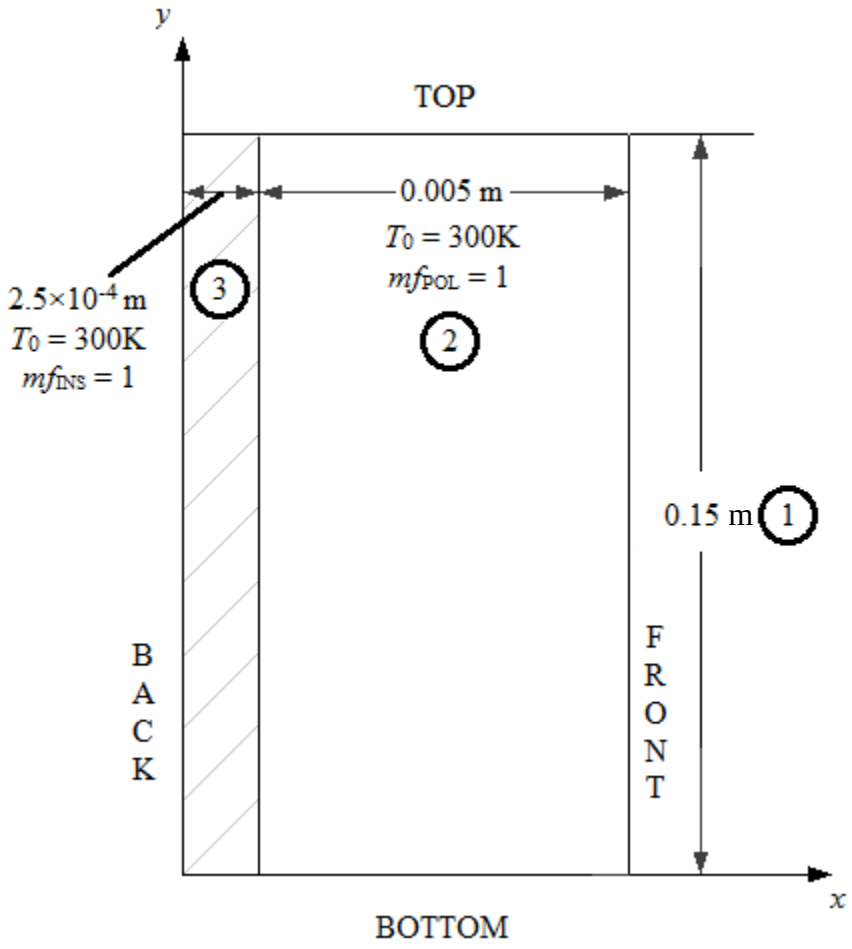

Figure 3. The 2D Object Defined by Example Conditions File (Circled numbers indicate sequence in which object sections are defined.)

OBJECT BOUNDARIES

FRONT BOUNDARY

MASS TRANSPORT: YES
GAS LIN 0.05 0 Equation 18: $J^{B}_{GAS} = 0.05\,\mathrm{m\,s^{-1}} \bullet \rho^{B}_{GAS}\left(\frac{\xi^{B}_{GAS}}{\rho^{B}_{GAS}} - 0\right)$

EXTERNAL HEAT FLUX 1: YES
START & END TIMES: 0 100
MODE: RAD
POSITION DEPEND1: 5e4 0 0.04
POSITION DEPEND2: 0 0 0
POSITION DEPEND3: 0 0 0

Equation 23:

$$D_0^1 = 50{,}000 \ \mathrm{W\,m^{-2}}$$
$$D_y^1 = 0 \qquad y_1 = 0.04\,\mathrm{m}$$
$$D_0^2 = D_y^2 = y_2 = 0$$
$$D_0^3 = D_y^3 = y_3 = 0$$

EXTERNAL HEAT FLUX 2: NO

FLAME: YES
IGNITION MASS FLUXES:
GAS 1e-3

Equation 22:

$$J_{\mathrm{GAS}}^{\mathrm{CI}} = 1\times10^{-3} \ \mathrm{kg\,s^{-1}\,m^{-2}}$$

FLAME LENGTH: 0.039 0.109 1

Equation 24:

$$Y_f = 0.039\mathrm{m} + 0.109\left(\int_0^Y \mathrm{CI}dy\right)^1$$

HEAT FLUX MODE: CONV
CONVECTION COEFF: 15

Equation 19:

$$hc = 15 \ \mathrm{W\,m^{-2}\,K^{-1}}$$

HEAT FLUX INSIDE: 2700 0.051 2300
HEAT FLUX BELOW: 100
HEAT FLUX ABOVE: 0.25 7.8 5.8

Equation 25:

$$D_f^1 = 2700\,\mathrm{K} \qquad y_f^s = 0.051\,\mathrm{m}$$
$$D_f^2 = 2300\,\mathrm{K} \qquad D_f^3 = 100\,\mathrm{m^{-2}}$$

Equation 26:

$$\Lambda = 0.25 + 7.8\exp\left(-5.8\,\mathrm{m^{-1}}\int_0^Y \mathrm{CI}dy\right)$$

BACKGROUND TEMP: 300 $\longrightarrow$ $T_b = 300\,\mathrm{K}$
RADIAT ABSORPT MODE: RAND

BACK BOUNDARY

MASS TRANSPORT: NO
EXTERNAL HEAT FLUX 1: NO
EXTERNAL HEAT FLUX 2: NO
FLAME: NO
BACKGROUND TEMP: 300
RADIAT ABSORPT MODE: MAX

INTEGRATION PARAMETERS

LAYER SIZE: 2e-4 $\longrightarrow$ $\Delta y = 2\times10^{-4}\,\mathrm{m}$
ELEMENT SIZE: 5e-5 $\longrightarrow$ $\Delta x = 5\times10^{-5}\,\mathrm{m}$
TIME STEP: 0.01 $\longrightarrow$ $\Delta t = 0.01\,\mathrm{s}$
DURATION: 250

OUTPUT FREQUENCY

LAYERS: 50
ELEMENTS: 10

TIME STEPS: 100

As in the case of 1D object input, turning off mass flow (MASS TRANSPORT: NO) at both boundaries also turns off all mass transfer inside the object. Turning off mass flow at one boundary turns off mass transfer in the *y*-direction. Layer and element size, timestep, and the length (DURATION) of simulation are followed by output frequencies. In the example shown above, information on the state of the object will be output every 100 timesteps. The output will include specification of location, temperature, and composition of every tenth element in every fiftieth layer of the object.

An example of a 1D object output file is given below. All information contained in this file is clearly defined and does not require any further explanation. Figure 4, which is included after the example 1D output file, helps to display how information is organized therein.

ThermaKin Program Version 3

Components file: i.cmp
Conditions file: i.cnd

Number of components: 3
Number of reactions: 1
Mixture rules assigned: yes

Object type: 1D

Top Boundary
External radiation: on
Mass transport: on
Ignition: off

Bottom Boundary
External radiation: off
Mass transport: off
Ignition: off

Started on: Mon Jul 02 17:30:20 2012

****

Time [s] = 0.000000e+000

BOUNDARY	AREA [m^2]	HEAT FLOW IN [J/s]	MASS FLOW OUT [kg/s]: POL	GAS	INS
TOP	1.000000e+000	4.360648e+004	0.000000e+000	0.000000e+000	0.000000e+000
BOTTOM	1.000000e+000	0.000000e+000	0.000000e+000	0.000000e+000	0.000000e+000

FROM TOP [m]	TEMPERATURE [K]	CONCENTRATION [kg/m^3]: POL	GAS	INS
2.500000e-005	3.000000e+002	1.300000e+003	0.000000e+000	0.000000e+000
5.250000e-004	3.000000e+002	1.300000e+003	0.000000e+000	0.000000e+000

1.025000e-003	3.000000e+002	1.300000e+003	0.000000e+000	0.000000e+000
1.525000e-003	3.000000e+002	1.300000e+003	0.000000e+000	0.000000e+000
2.025000e-003	3.000000e+002	1.300000e+003	0.000000e+000	0.000000e+000
2.525000e-003	3.000000e+002	1.300000e+003	0.000000e+000	0.000000e+000
3.025000e-003	3.000000e+002	1.300000e+003	0.000000e+000	0.000000e+000
3.525000e-003	3.000000e+002	1.300000e+003	0.000000e+000	0.000000e+000
4.025000e-003	3.000000e+002	1.300000e+003	0.000000e+000	0.000000e+000
4.525000e-003	3.000000e+002	1.300000e+003	0.000000e+000	0.000000e+000
5.025000e-003	3.000000e+002	0.000000e+000	0.000000e+000	1.000000e+002
5.225000e-003	3.000000e+002	0.000000e+000	0.000000e+000	1.000000e+002

Total thickness [m] = 5.250000e-003
Total mass [kg/m^2] = 6.525000e+000

****

Time [s] = 1.000000e+000

BOUNDARY	AREA [m^2]	HEAT FLOW IN [J/s]	MASS FLOW OUT [kg/s]: POL	GAS	INS
TOP	1.000000e+000	4.342140e+004	0.000000e+000	0.000000e+000	0.000000e+000
BOTTOM	1.000000e+000	0.000000e+000	0.000000e+000	0.000000e+000	0.000000e+000

FROM TOP [m]	TEMPERATURE [K]	CONCENTRATION [kg/m^3]: POL	GAS	INS
2.500000e-005	3.281488e+002	1.300000e+003	0.000000e+000	0.000000e+000
5.250000e-004	3.089813e+002	1.300000e+003	0.000000e+000	0.000000e+000
1.025000e-003	3.005103e+002	1.300000e+003	0.000000e+000	0.000000e+000
1.525000e-003	3.001671e+002	1.300000e+003	0.000000e+000	0.000000e+000
2.025000e-003	3.000088e+002	1.300000e+003	0.000000e+000	0.000000e+000
2.525000e-003	3.000001e+002	1.300000e+003	0.000000e+000	0.000000e+000
3.025000e-003	3.000000e+002	1.300000e+003	0.000000e+000	0.000000e+000
3.525000e-003	3.000000e+002	1.300000e+003	0.000000e+000	0.000000e+000
4.025000e-003	3.000000e+002	1.300000e+003	0.000000e+000	0.000000e+000
4.525000e-003	3.000000e+002	1.300000e+003	0.000000e+000	0.000000e+000
5.025000e-003	3.000000e+002	0.000000e+000	0.000000e+000	1.000000e+002
5.225000e-003	3.000000e+002	0.000000e+000	0.000000e+000	1.000000e+002

Total thickness [m] = 5.250000e-003
Total mass [kg/m^2] = 6.525000e+000

•••

•

•

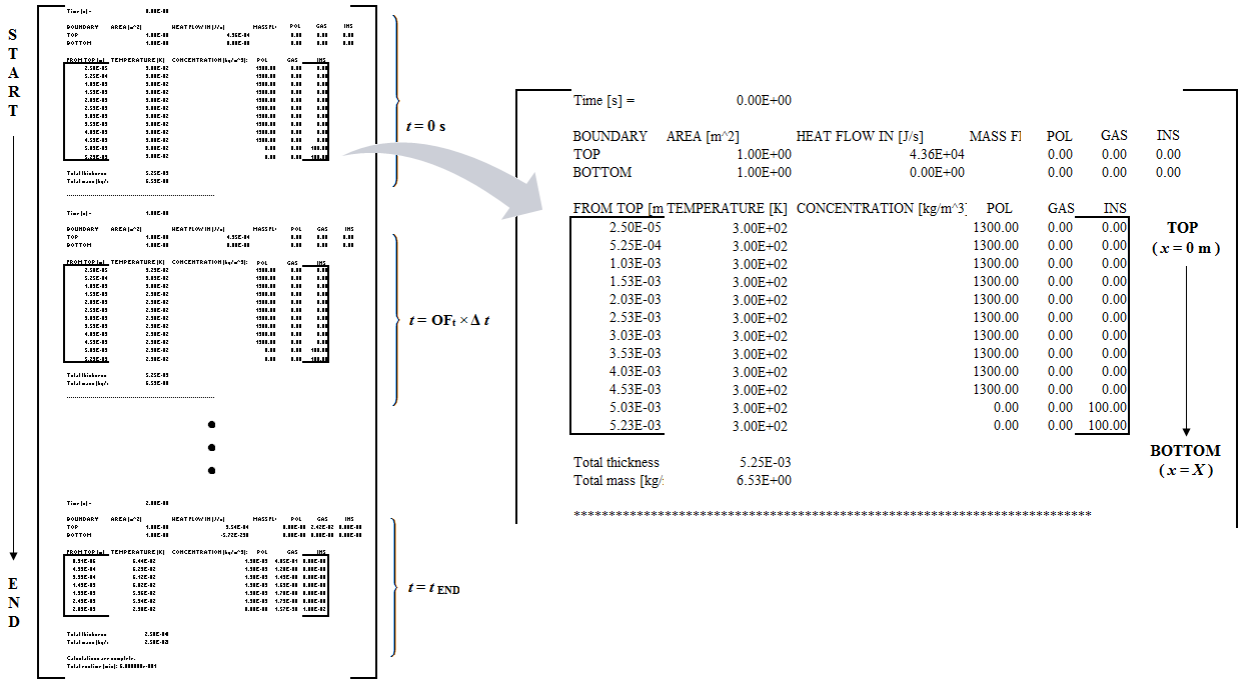

Figure 4. Organization of ThermaKin Output File From a 1D Object Simulation (OF indicates output frequency.)

An example 2D object output file is given below. Flame position (FLAME POS) indicates y position of the edge of the ignited surface closest to the bottom (y = 0). Figure 5, which is included after the 2D output file, is included as a reference to display how information is organized therein.

ThermaKin Program Version 3

Components file: i.cmp
Conditions file: i2D.cnd

Number of components: 3
Number of reactions: 1
Mixture rules assigned: yes

Object type: 2D
Number of layers: 750

Front Boundary
External heating: on
Mass transport: on
Ignition: on

Back Boundary
External heating: off
Mass transport: off
Ignition: off

Started on: Fri Jun 29 18:48:12 2012

****

Time [s] = 0.000000e+000

BOUNDARY	AREA [m^2]	FLAME POS [m]	HEAT FLOW IN [J/s]	MASS FLOW OUT [kg/s]: POL	GAS	INS
FRONT	1.500000e-001	- No Flame --	1.321601e+003	0.000000e+000	0.000000e+000	0.000000e+000
BACK	1.500000e-001	- No Flame --	0.000000e+000	0.000000e+000	0.000000e+000	0.000000e+000

FROM BOTTOM [m] = 1.000000e-004

FROM BACK [m]	TEMPERATURE [K]	CONCENTRATION [kg/m^3]: POL	GAS	INS
5.225000e-003	3.000000e+002	1.300000e+003	0.000000e+000	0.000000e+000
4.725000e-003	3.000000e+002	1.300000e+003	0.000000e+000	0.000000e+000
4.225000e-003	3.000000e+002	1.300000e+003	0.000000e+000	0.000000e+000
3.725000e-003	3.000000e+002	1.300000e+003	0.000000e+000	0.000000e+000
3.225000e-003	3.000000e+002	1.300000e+003	0.000000e+000	0.000000e+000
2.725000e-003	3.000000e+002	1.300000e+003	0.000000e+000	0.000000e+000
2.225000e-003	3.000000e+002	1.300000e+003	0.000000e+000	0.000000e+000
1.725000e-003	3.000000e+002	1.300000e+003	0.000000e+000	0.000000e+000
1.225000e-003	3.000000e+002	1.300000e+003	0.000000e+000	0.000000e+000
7.250000e-004	3.000000e+002	1.300000e+003	0.000000e+000	0.000000e+000
2.250000e-004	3.000000e+002	0.000000e+000	0.000000e+000	1.000000e+002
2.500000e-005	3.000000e+002	0.000000e+000	0.000000e+000	1.000000e+002

Thickness [m] = 5.250000e-003
Mass [kg/m^2] = 6.525000e+000

FROM BOTTOM [m] = 1.010000e-002

FROM BACK [m]	TEMPERATURE [K]	CONCENTRATION [kg/m^3]: POL	GAS	INS
5.225000e-003	3.000000e+002	1.300000e+003	0.000000e+000	0.000000e+000
4.725000e-003	3.000000e+002	1.300000e+003	0.000000e+000	0.000000e+000
4.225000e-003	3.000000e+002	1.300000e+003	0.000000e+000	0.000000e+000
3.725000e-003	3.000000e+002	1.300000e+003	0.000000e+000	0.000000e+000
3.225000e-003	3.000000e+002	1.300000e+003	0.000000e+000	0.000000e+000
2.725000e-003	3.000000e+002	1.300000e+003	0.000000e+000	0.000000e+000
2.225000e-003	3.000000e+002	1.300000e+003	0.000000e+000	0.000000e+000
1.725000e-003	3.000000e+002	1.300000e+003	0.000000e+000	0.000000e+000
1.225000e-003	3.000000e+002	1.300000e+003	0.000000e+000	0.000000e+000
7.250000e-004	3.000000e+002	1.300000e+003	0.000000e+000	0.000000e+000
2.250000e-004	3.000000e+002	0.000000e+000	0.000000e+000	1.000000e+002
2.500000e-005	3.000000e+002	0.000000e+000	0.000000e+000	1.000000e+002

Thickness [m] = 5.250000e-003
Mass [kg/m^2] = 6.525000e+000

•••

•

•

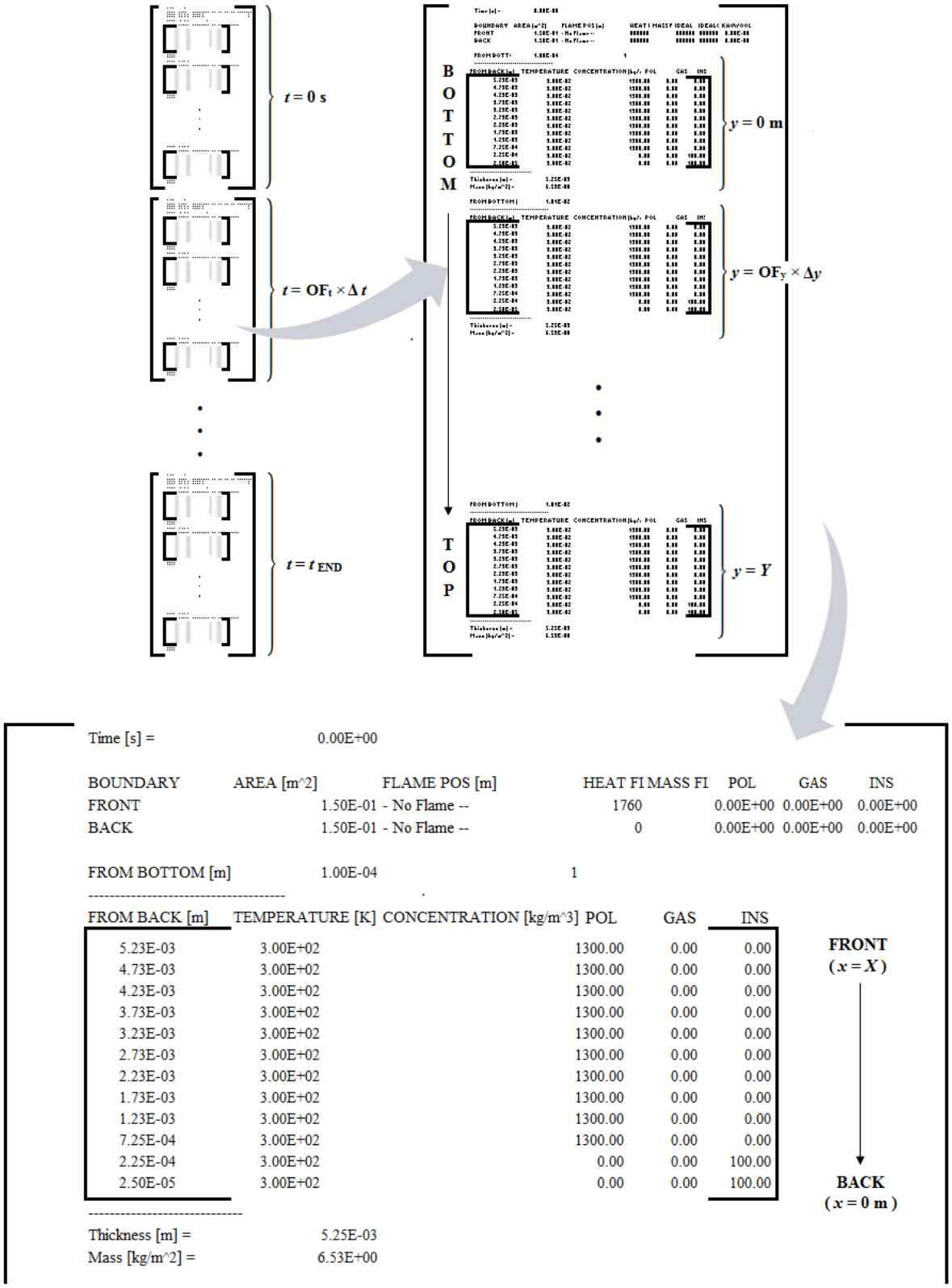

Figure 5. Organization of ThermaKin Output File From a 2D Object Simulation (OF indicates output frequency.)

MODEL VERIFICATION

With the exception of very minor changes in the boundary condition formulation, a 1D object model within ThermaKin2D is identical to that implemented in ThermaKin. The accuracy of this model was verified by comparing conductive and radiative transfer, mass transport, and chemical reaction simulations to the corresponding analytical solutions [4]. This model was also shown to be able to capture experimentally observed burning behavior of a wide range of materials [6,7, and 20].

The fact that a 1D object model within ThermaKin2D is fully validated made it possible to use it for verification of a 2D object model. Heat and mass transfer and complete pyrolysis in a 2D object were simulated using initial and boundary conditions imposing a 1D problem geometry (for each of the two dimensions). The results of these simulations were compared with the results of the actual 1D object simulations. A considerable effort was made to understand how the accuracy of the solution is affected by the choice of integration parameters and what limitations are imposed by the explicit integration used for one of the 2D object dimensions. The results of these efforts and a demonstration of the application of ThermaKin2D to an upward flame-spread problem are described below.

HEAT TRANSFER.

All simulations were performed using material properties that are typical for a synthetic polymer used in transportation and building applications. The physical property set, which is summarized in table 1, was obtained by averaging property values of as many as 97 polymeric materials [21]. Several heat transfer scenarios were examined.

Table 1. Physical Properties of a Typical Synthetic Polymer

Property	Value
ρ	1.3×10^{3} kg m^{-3}
c	2.3×10^{3} J kg^{-1} K^{-1}
k	0.24 W m^{-1} K^{-1}
α	2.9 m^{2} kg^{-1}
ε	0.88

In the first scenario, one face of 5×10^{-3}-m-thick material plate was subjected to uniform radiative and convective heat fluxes for 360 s. The incident radiation was set at 2.5×10^{4} W m^{-2}; the convection was defined by hc = 15 W m^{-2} K^{-1} and T^{e} = 1965 K. The absorption and emission of radiation were computed using the random-absorption algorithm. The other face and sides of the plate were perfectly insulated. The initial temperature of the plate was set at 300 K.

The calculation was first performed with a 1D (fully validated) model using $\Delta x = 1\times10^{-5}$ m and Δt = 0.01 s. The results are shown in figure 6. This calculation was subsequently repeated with both element size and timestep reduced by an order of magnitude. The latter calculation showed no significant differences from the former one (see figure 6) indicating that a combination of $\Delta x = 1\times10^{-5}$ m and Δt = 0.01 s results in a converged solution for heat flow. Further analysis

revealed that increasing either Δx or Δt produces gradually increasing deviations of temperature from the converged values. At $\Delta x = 1\times10^{-4}$ m and $\Delta t = 0.1$ s, these deviations are still relatively small; the time-averaged relative difference (with respect to the fully converged simulation) was found to be below 0.5% throughout the plate thickness. At $\Delta x = 1\times10^{-3}$ m and $\Delta t = 0.1$ s, these deviations become more notable, around 2%.

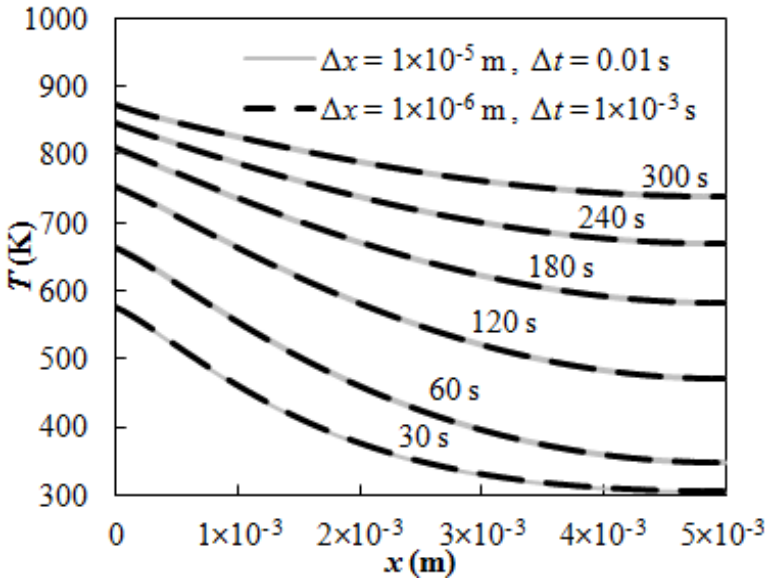

Figure 6. Temperature Evolution inside 5×10^{-3}-m-Thick, Inert-Material Plate Heated on One Side with a Combination of Convective and Radiative Heat Fluxes

The same heat transfer scenario was implemented in the 2D model. The plate was set to be $50\times\Delta y$ long. The heat-exposed face of the plate was represented by the front boundary (see figure 1), which aligned the heat-flow vector with x (semi-implicitly integrated) direction. Using $\Delta x = \Delta y = 1\times10^{-5}$ m and $\Delta t = 0.01$ s resulted in a complete divergence of the simulation (the temperature values were outside the numerical range allowable by the compiler). A thorough examination revealed that to avoid divergence, the ratio of $(\Delta y)^2$ and Δt should be kept above 2×10^{-7} m^2 s^{-1} (a limitation believed to be imposed by the explicit integration in the y direction). Furthermore, as long as this ratio was set above the recommended threshold, the selection of Δy had no impact on the resulting temperature histories. These histories were essentially identical to those obtained with the 1D model (at the same Δx and Δt settings).

In the second heat transfer scenario, the top 5×10^{-4}-m-thick slice of 5×10^{-3}-m-thick material plate was heated instantaneously to 1000 K at $t = 0$. The rest of the plate was initially 300 K. The plate was perfectly insulated on all sides. Using the 2D model, 240 s of the plate temperature history was computed. The steplike initial temperature profile was first aligned with x-coordinate and, subsequently, with y-coordinate. The results of the simulations shown in figure 7 indicate that, at $\Delta x = \Delta y = 5\times10^{-5}$ m and $\Delta t = 0.01$ s, x and y (i.e., semi-implicit and explicit) integration procedures produce identical converged results.

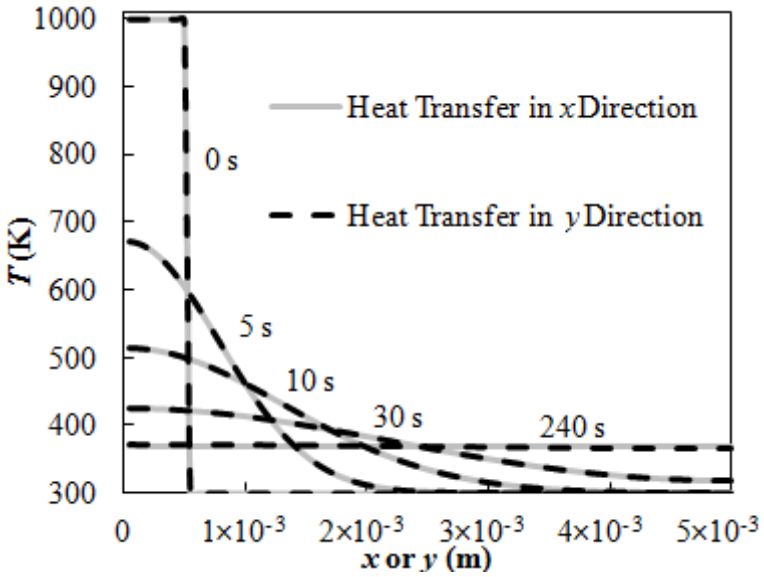

Figure 7. Thermal Wave Propagation inside 5×10^{-3}-m-Thick, Inert-Material Plate Computed With the 2D Model

The final heat-transfer scenario was used to examine the 2D propagation of thermal energy through the material. A square material object, 5×10^{-3} by 5×10^{-3} m in size, was subjected to an instantaneous temperature perturbation at t = 0 where 5×10^{-4}-by 5×10^{-4}-m-corner area of the square was heated to 1000 K, while the rest of the object was at 300 K. The object was perfectly insulated on all sides. Its temperature was tracked for 300 s using a 2D model and the same integration parameter values as those used to simulate the second scenario. The results of the simulations are shown in figure 8. These results show expected symmetry and equilibrium temperature convergence that corresponds to complete conservation of energy. Overall, these exercises indicate that, for a typical material combustion scenario, ThermaKin2D ran using 5×10^{-5}-m spatial discretization and a 0.01-s timestep produces an accurate solution for heat transfer.

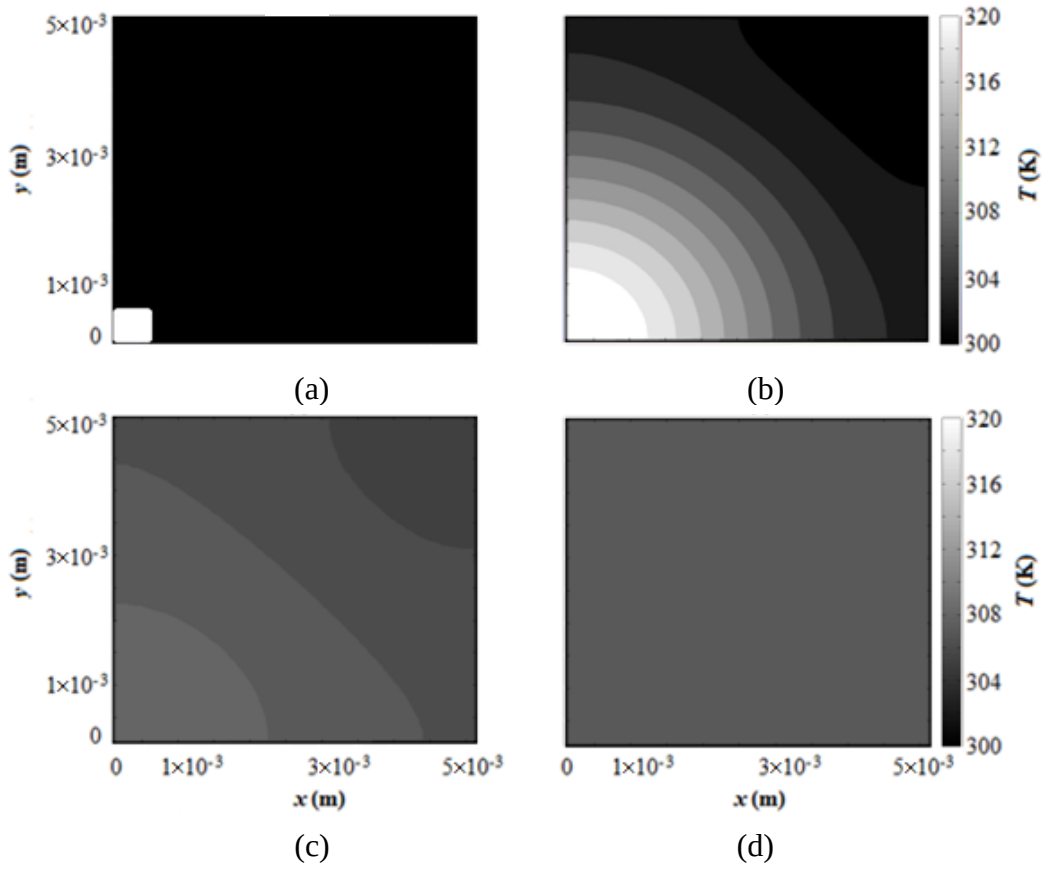

Figure 8. The 2D Thermal Wave Propagation Inside Square (5×10^{-3}-by 5×10^{-3}-m) Material Object (The temperature profiles are reported at (a) t = 0, (b) t = 30, (c) t = 90, and (d) t = 300 s.)

MASS TRANSFER.

Relatively little is known about the rates of transfer of gaseous thermal degradation products inside pyrolyzing solids. Some evidence indicates that these rates are relatively high and, therefore, are not burning-rate limiting [7]. Here, it is assumed that this transfer can be described by $\lambda = 1\times10^{-5}$ m^2 s^{-1}, which has the same magnitude as the diffusion coefficients of diatomic gases in the air at atmospheric pressure and room temperature. This gas transfer coefficient is likely to represent the upper bound of possible values.

The density of the solid material was specified to be equal to that given in table 1. All gas properties were assumed to be equal to the properties of the solid. The γ_s was set to 0, which means that the gas did not contribute to the material volume and, therefore, its density was irrelevant. Two mass transfer scenarios were examined. In both scenarios, all heat transfer was turned off.

In the first scenario, the top 1×10^{-3}-m-thick slice of 1×10^{-2}-m-thick, solid-material plate was set to contain 1% (by mass) of the gaseous component at t = 0. The rest of the plate was initially set to be free of gas. All plate boundaries were specified to be impenetrable to gas flow. The gas mass fraction evolution was first computed using the 1D (fully validated) model. The results

obtained using $\Delta x = 1\times10^{-5}$ m and $\Delta t = 0.01$ s are shown in the left graph in figure 9. It appears that the integration discretization, which was more than sufficient to provide a fully converged solution for the heat transfer, fails to provide convergence in the case of mass transfer (probably because of higher rate of this process). This calculation produced an unrealistic gas mass fraction spike, which is reduced with time and disappears at about 1 s (the system reached equilibrium at about 5 s). Reducing timestep by a factor of ten essentially eliminated this spike and produced a converged solution, as evidenced by the results shown by the right graph in figure 9. Raising Δx to 1×10^{-4} or 1×10^{-3} m, while keeping the ratio of element size and timestep at 0.01 m s^{-1}, generated results that were still, on average, within 1% of the completely converged $\Delta x = 1\times10^{-5}$ m and $\Delta t = 1\times10^{-4}$ s calculations.

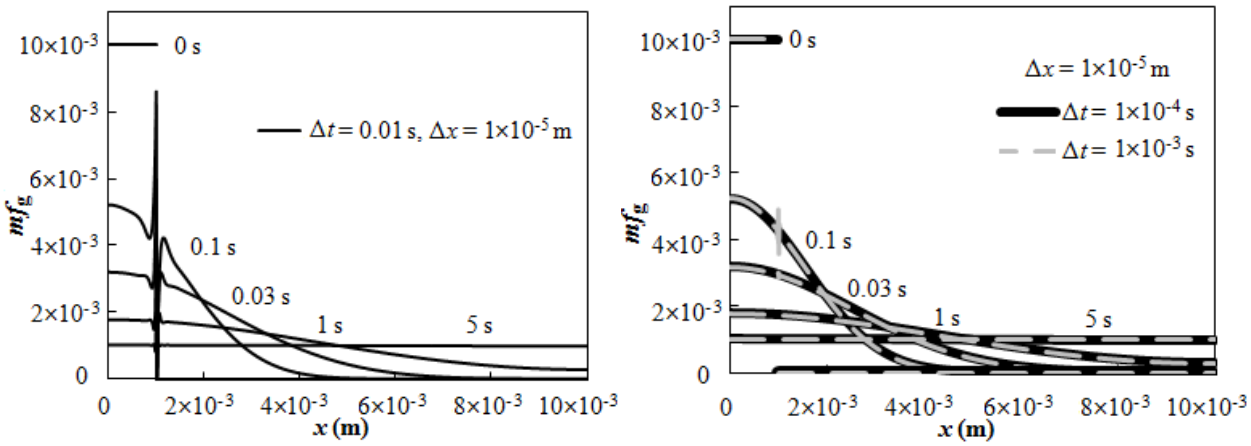

Figure 9. Gas Propagation inside 1×10^{-2}-m-Thick, Inert-Material Plate Computed With the 1D Model

The same mass-transfer scenario was implemented in the 2D model. The plate was set to be $50\times\Delta y$ long. The model was set up in such a way that the direction of gas transfer was aligned with x (semi-implicitly integrated) coordinate. Using $\Delta x = \Delta y = 1\times10^{-5}$ m and $\Delta t = 1\times10^{-3}$ s resulted in a complete divergence of the simulation (the gas mass fractions were found to be outside a physically meaningful range of values). As in the case of heat transfer, it was subsequently established that, to avoid divergence, the ratio of $(\Delta y)^2$ and Δt had to be kept above a certain threshold, 2×10^{-5} m^2 s^{-1}. Provided that this condition was satisfied, the selection of Δy had no impact on the resulting mass-fraction histories. These histories were essentially identical to those obtained with the 1D model (at the same Δx and Δt settings).

In the next 2D model simulation, the steplike initial gas mass fraction profile was aligned with y coordinate. A comparison of this simulation results in the x coordinate mass transfer dynamics obtained using the same discretization, $\Delta x = \Delta y = 5\times10^{-5}$ m and $\Delta t = 1\times10^{-4}$ s, as shown in figure 10. This comparison indicates that, with properly selected integration parameters, x and y (i.e., semi-implicit and explicit) integration procedures produce identical converged results.

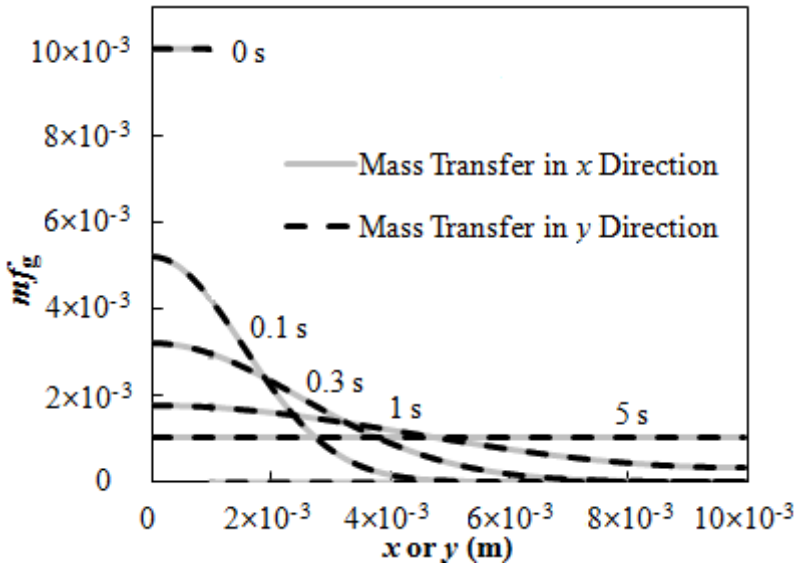

Figure 10. Gas Propagation inside 1×10^{-2}-m-Thick, Inert-Material Plate Computed With the 2D Model

The second mass-transfer scenario was used to examine 2D transport. A 5×10^{-4}- by 5×10^{-4}-m corner area of 5×10^{-3}- by 5×10^{-3}-m-square, solid-material object was seeded with 1% of gas at t = 0. All object boundaries were specified to be impenetrable to gas flow. The results of this simulation, performed using $\Delta x = \Delta y = 5\times10^{-5}$ m and $\Delta t = 1\times10^{-4}$ s, are shown in figure 11. These results show expected symmetry and equilibrium mass fraction convergence that corresponds to complete conservation of mass.

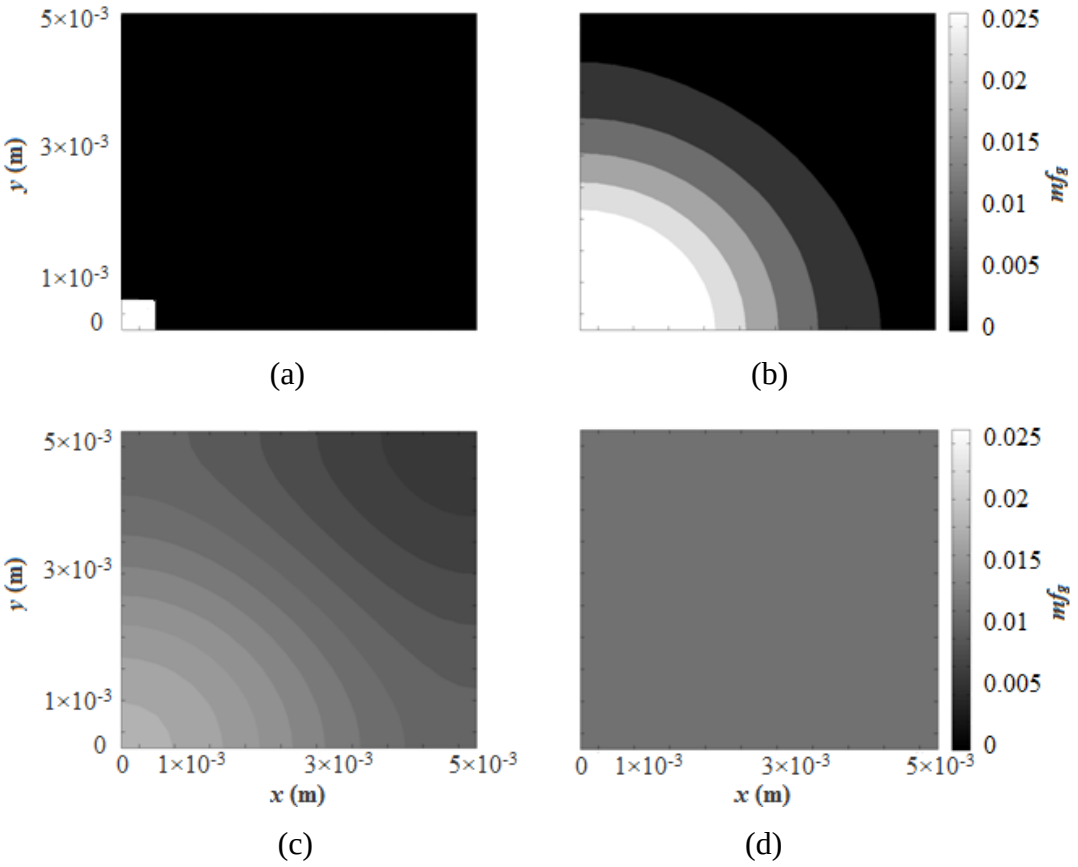

Figure 11. Two-Dimensional Gas Propagation Inside Square (5×10^{-3} by 5×10^{-3}-m) Inert Material Object. (The mass concentration profiles are reported at (a) t = 0 s, (b) t = 0.2 s, (c) t = 0.6 s, and (d) t = 2.0 s.)

Overall, these mass transfer simulations indicate that ThermaKin2D can capture this phenomenon accurately. However, the timestep required to obtain fully converged mass transport dynamics in the presence of high-concentration gradients is about two orders of magnitude smaller than that recommended for heat transport. For example, 5×10^{-5}-m spatial discretization requires $\Delta t = 1\times10^{-4}$ s.

BURNING RATE.

Material burning was also simulated in two scenarios. The physical properties of the initial (solid) material were set to be equal to those specified in table 1. This material was assumed to degrade to gas through a single first-order reaction. The parameters describing this reaction, $A = 1.6\times10^{16}$ s^{-1}, $E = 2.18\times10^{5}$ J mol^{-1}, and $h = -1.3\times10^{6}$ J kg^{-1} (endothermic), were obtained by averaging degradation kinetics and thermodynamics of as many as 35 polymers [21]. The stoichiometric coefficients for the reactant and product were set to unity. The physical properties of the gas were assumed to be equal to the properties of the solid. The γ_s was set to 0, which means the gas did not contribute to the material volume. The gas transport coefficient was kept at 1×10^{-5} m^2 s^{-1}.

In the first scenario, one face of a 5×10^{-3}-m-thick, solid-material plate was subjected to 5.0×10^{4} W m^{-2} of incident radiative heat flux for 500 s. This face was also specified to be transparent to gas flow (a and b in the linear form of equation 18 were set to 0.05 m s^{-1} and 0, respectively). The other face and sides of the plate were defined to be impenetrable to heat or gas. The initial temperature of the plate was set at 300 K.

The first calculation was performed with a 1D (fully validated) model using $\Delta x = 5\times10^{-5}$ m and $\Delta t = 0.01$ s. According to the simulations discussed above, these integration parameters produce a converged solution for heat transport in a similar scenario. It was assumed that these parameters also provide adequate resolution for gas transport because, unlike in the case of the mass transport scenario analyzed above, the gas forms gradually and, as a result, its transport is driven by much smaller concentration gradients. The results shown in figure 12 confirm that these integration parameters provide a converged solution. The mass loss or burning rate (normalized per-unit area of the heat-exposed face of the plate) does not change significantly when either Δx or Δt is increased by a factor of 5. The presence of noise on these burning rate curves is a manifestation of the application of the random-absorption algorithm (which was used to handle absorption and emission of the radiation transferring through the plate face).

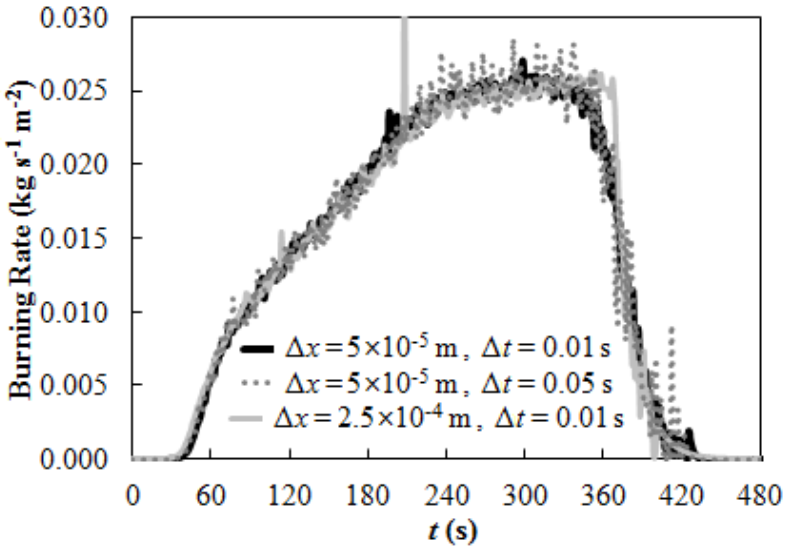

Figure 12. Burning-Rate History of 5×10^{-3}-m-Thick, Solid-Material Plate Exposed to 5.0×10^{4} W m^{-2} of Radiative Heat (All curves are computed using the 1D model.)

The same burning scenario was implemented in a 2D model. The plate was set to be $50\times\Delta y$ long. The heat-exposed face of the plate was represented by the front boundary (see figure 1), which aligned the heat-flow vector with x-direction. The gas transport was limited to this direction. The results of the calculations obtained using $\Delta x = 5\times10^{-5}$ m, $\Delta y = 2\times10^{-4}$ m, and $\Delta t = 0.01$ s are compared with the converged 1D model simulation in figure 13. These curves are essentially identical, which means that the heat and mass transfer coupled with chemical kinetics are solved correctly by ThermaKin2D. The 2D results show no noise because the mass loss rate is averaged over 50 surface elements. Increasing any of the integration parameters by a factor of 5 did not produce significant changes in the results of the 2D simulations.

In the second scenario, upward flame spread on a 0.15-m-tall and 5×10^{-3}-m-thick solid-material plate was examined. The initial temperature of the plate was set at 300 K. To ignite the flame, the bottom 0.03 m of the front face of the plate was irradiated with 5.0×10^{4} W m^{-2} of incident heat flux for 43 s. This face was also specified to be transparent to gas flow. The critical (ignition) gas flux was set at 1×10^{-3} kg s^{-1} m^{-2}. The back and sides of the plate were defined to be impenetrable to heat or gas.

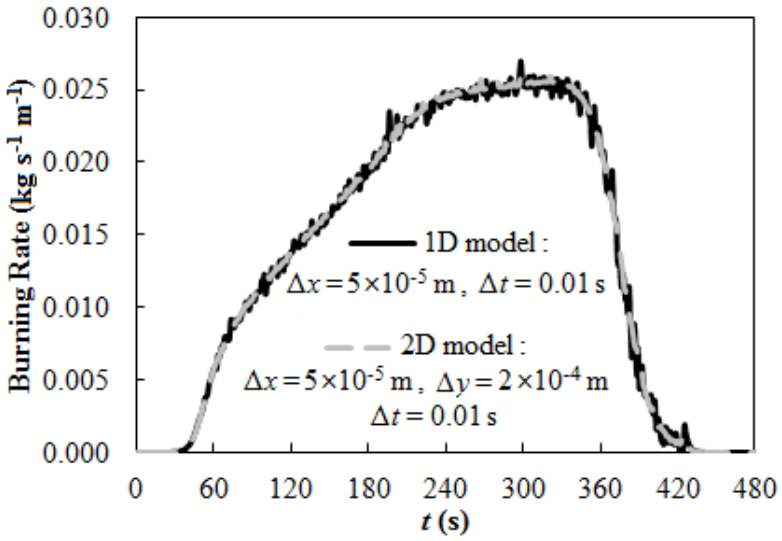

Figure 13. Comparison of the 1D and 2D Models, Calculations of Burning of 5×10^{-3}-m-Thick, Solid-Material Plate Exposed to 5.0×10^{4} W m^{-2} of Radiative Heat

The heat flux from the flame to material was assumed to be convective in nature. This heat flux (q_f) was formulated as:

$$q_f = hc_f\left(D_f + T_b - T^{\mathrm{B}}\right) \tag{27}$$

where D_f (representing environmental temperature) and T^{B} (representing material surface temperature) are functions of y. The parameters used to compute this heat flux, including the parameters of D_f function defined by equations 24 through 26, are provided in table 2. These parameters were obtained from recent experimental measurements of the heat feedback from a flame spreading vertically on poly(methyl methacrylate) [14]. Note that this is the only scenario examined in this study in which the background temperature (T_b) was specified to be above 0.

This flame-spread scenario was implemented in the 2D model and solved using $\Delta x = 5\times10^{-5}$ m, $\Delta y = 2\times10^{-4}$ m, and $\Delta t = 0.01$ s. As in the previously described simulations of burning, the gas transport was limited to x-direction. The computed evolution of the flame heat-flux profile is shown in figure 14. The flame, which is anchored to the bottom of the plate ($y = 0$), ignites a few seconds before removal of the radiative heat source and grows with time. A more detailed illustration of fire dynamics is captured by the plate's burning rate, which was normalized by the width of the plate, as shown in figure 15. The sharp increase in the burning rate associated with

the ignition of the flame is followed by a drop associated with the removal of the radiative heat source. The subsequent rise in burning rate reflects the flame's upward spread, covering a larger and larger area of the plate. This rise has an expected, nonlinear profile. Increasing any of the integration parameters by a factor of 5 did not produce significant changes in the results of this simulation, indicating a converged solution.

Table 2. Parameters Describing Heat Flow From Flame to Material Surface

Parameter	Value
Y_f^0	0.039 m
Y_f^{CI}	0.109
Y_f^{PW}	1
D_f^1	2.7×10^3 K
D_f^2	2.3×10^3 K
D_f^3	100 m^{-2}
y_f^s	0.051 m
Λ_0	0.25
Λ_{CI}	7.8
Λ_{ex}	5.8 m^{-1}
T_b	300 K
hc_f	15 $\mathrm{W\,m^{-2}\,K^{-1}}$

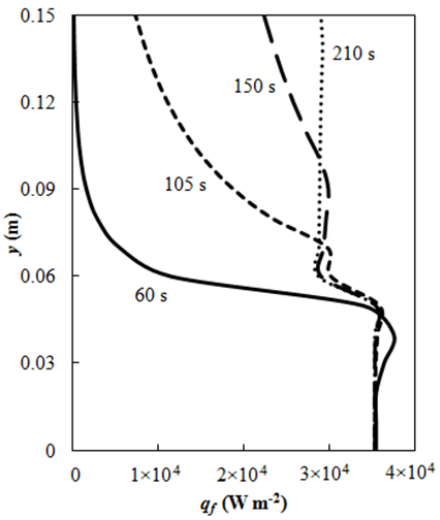

Figure 14. Evolution of Flame Spreading Upward on 0.15-m-Tall and 5×10^{-3}-m-Thick, Solid-Material Plate

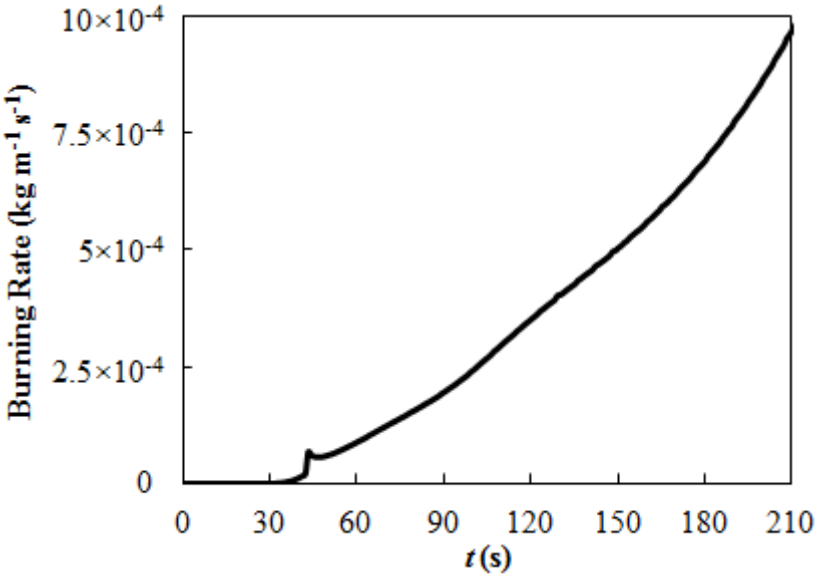

Figure 15. Burning Rate of 0.15-m-Tall and 5×10^{-3}-m-Thick, Solid-Material Plate Ignited With a Radiant Heat Source and in Upward Flame Spread

CONCLUSIONS

A new computational tool, ThermaKin2D, has been formulated, coded, and verified. This tool extends pyrolysis modeling to a two-dimensional system. A flexible boundary condition formalism implemented in this tool provides a capability to couple pyrolysis with detailed analytical representations of the energy feedback from surface flames, which produces a robust simulator of flame-spread on material surfaces. The future work will be focused on examining the ability of this tool to predict experimentally observed burning dynamics. It is expected that this tool will help reconcile frequently contradictory material flammability assessments based on constant-burning area and flame-spreading scenarios.

REFERENCES

1. Kashiwagi, T., "Polymer Combustion and Flammability—Role of the Condensed Phase," *Twenty-Fifth Symposium (International) on Combustion*, 1994, pp. 1423-1437.

2. Lautenberger, C. and Fernandez-Pello, C., "Generalized Pyrolysis Model for Combustible Solids," *Fire Safety Journal*, Vol. 44, 2009, pp. 819-839.

3. McGrattan, K., Hostikka, S., Floyd, J., Baum, H., Rehm, R., Mell, W., and McDermott, R., "Fire Dynamics Simulator (Version 5) Technical Reference Guide," National Institute of Standards and Technology Special Publication, 2007.

4. Stoliarov, S.I. and Lyon, R.E., "Thermo-Kinetic Model of Burning," Federal Aviation Administration Technical Note, DOT/FAA/AR-TN08/17, 2008.

5. 2012 American Chemical Society Spring National Meeting, *Fire and Polymers Symposium*, San Diego, California, March 2012.

6. Stoliarov, S.I., Crowley, S., Lyon, R.E., Linteris, G.T., "Prediction of the Burning Rates of Non-Charring Polymers," *Combustion and Flame*, Vol. 156, 2009, pp. 1068-1083.

7. Stoliarov, S.I., Crowley, S., Walters, R.N., Lyon, R.E., "Prediction of the Burning Rates of Charring Polymers," *Combustion and Flame*, Vol. 157, 2010, pp. 2024-2034.

8. ASTM E 1354 – 09, "Standard Test Method for Heat and Visible Smoke Release Rates for Materials and Products Using an Oxygen Consumption Calorimeter," ASTM International, West Conshohocken, Pennsylvania, 2009.

9. Quintiere, J.G., *Fundamentals of Fire Phenomena*, John Wiley & Sons, Chichester, United Kingdom, 2006.

10. De Ris, J.N., "Spread of Laminar Diffusion Flame," *Twelfth Symposium (International) on Combustion*, 1969, pp. 241-252.

11. Fernandez-Pello, A.C., Hirano, T., "Controlling Mechanisms of Flame Spread," *Combustion Science and Technology*, Vol. 32, 1983, pp. 1-31.

12. Quintiere, J., Harkleroad, M., Hasemi, Y., "Wall Flames and Implications for Upward Flame Spread," *Combustion Science and Technology*, Vol. 48, 1986, pp. 191-222.

13. Ito, A., Kashiwagi, T., "Characterization of Flame Spread over PMMA Using Holographic Interferometry Sample Orientation Effects," *Combustion and Flame*, Vol. 71, 1988, pp. 189-204.

14. Leventon, I.T., Stoliarov, S.I., "Evolution of Flame to Surface Heat Flux During Upward Flame Spread on Poly(methyl methacrylate)," *Proceedings of the Combustion Institute*, in press.

15. Holman, J.P., *Heat Transfer, Ninth Edition*, McGraw-Hill, Boston, Massachusetts, 2002.

16. Siegel, R., Howell, J., *Thermal Radiation Heat Transfer, Fourth Edition*, Taylor & Francis, New York, New York, 2002.

17. Scheidegger, A.E., *The Physics of Flow Through Porous Media*, University of Toronto Press, Toronto, Canada, 1974, pp. 73-98.

18. Blinder, S.M., *Advanced Physical Chemistry: A Survey of Modern Theoretical Principles*, The Macmillan Company, London, United Kingdom, 1969.

19. Press, W.H., Teukolsky, S.A., Vetterling, W.T., Flannery, B.P., *Numerical Recipes in C++: The Art of Scientific Computing,* Cambridge University Press, Cambridge, United Kingdom, 2002.

20. Kempel, F., Schartel, B., Linteris, G.T., Stoliarov, S.I., Lyon, R.E., Walters, R.N., Hofmann, A., "Prediction of the Mass Loss Rate of Polymer Materials: Impact of Residue Formation," *Combustion and Flame,* in press.

21. Stoliarov, S.I., Safronava, N., Lyon, R.E., "The Effect of Variation in Polymer Properties on the Rate of Burning," *Fire and Materials,* Vol. 33, 2009, pp. 257-271.